Proceedings of the
Annual Stability Conference
Structural Stability Research Council
Grapevine, Texas, April 18-21, 2012

Instabilities of cellular members loaded in bending or compression

D. Sonck[1], N. Boissonnade[2], R. Van Impe[3]

Abstract
Cellular members are I-section steel members with evenly spaced round web openings. The main advantage these members have over plain-webbed I-section members is their optimized material use in strong-axis bending. Consequently, they are principally used for applications in which they are loaded in bending, but they are also applied in cases where they are subjected to a combination of a compressive force and a bending moment. For cellular members loaded in bending, the current design approaches for global buckling give conflicting results, while for compressed cellular members and members loaded in compression and bending, research is lacking altogether. Before research can start on the last load combination, both extreme load cases of bending moment and normal force alone should be investigated first. In this paper, the global buckling behaviour of cellular members loaded in compression or bending will be investigated. For the bending moment load case, the most promising existing approach will be examined, as well as slight alterations to this approach. For the normal force load case, a new approach, based on the bending moment approach, will be proposed and examined. Based on the comparison of these approaches with results from numerical simulations for a wide variety of cellular beam geometries, the design approaches that give the best results will be determined.

1. Introduction

Cellular members are steel I-section members with evenly spaced round web openings, made from hot-rolled I-section members (Fig. 1). Compared with beams without web openings of the same weight, the bending resistance and stiffness of cellular beams will be considerably higher. Alternatively put, for beams spanning the same length, the weight of the cellular member will be much lower. Other than this economic material use, cellular members have some further advantages. Service ducts can be guided through the openings in the beams instead of under the beams, thus decreasing the total construction height of the building. Additionally, cellular members have a lighter appearance, which may also be an advantage from an aesthetic point of view.

Cellular members are mostly used for applications in which they are loaded in strong-axis bending, their increased bending resistance being their major advantage. However, they are also used in applications in which they are subjected to a combination of a (relatively large) bending

[1] PhD Student, Ghent University, <Delphine.Sonck@UGent.be>
[2] Professor, College of Engineering and Architecture of Fribourg, < Nicolas.Boissonnade@hefr.ch >
[3] Professor, Ghent University, <Rudy.VanImpe@UGent.be>

moment and a compressive force. Additionally, they can have tapered or curved shapes, and they can also be used in steel-concrete composite structures. An overview of some cellular member applications is given in Fig. 1.

Figure 1. Cellular beam applications

The global buckling behavior of cellular members loaded by a combination of a compressive force (N) and a strong-axis bending moment (M) will differ from the behavior of members without web openings. However, to the authors' best knowledge currently no research exists on this subject. Even for the extreme load cases of only compression (N) or bending (M) and the most basic boundary condition of a simply supported member, results are limited. For compressed members, no research exists for the governing instability mode of weak-axis buckling. For cellular beams loaded in strong-axis bending, some research exists and two design approaches are currently used (cf. §3). However, these lead to conflicting results. The first design approach is overly safe and hence uneconomic, while the second design approach is not very well defined and could possibly lead to unsafe results. Consequently, even for the most basic two load cases mentioned above research is lacking.

The subject of global buckling failure of cellular members in compression and bending is currently being investigated by the authors. In this paper, the results of a small part of this research will be presented: the global buckling behavior of members loaded in strong-axis bending or compression. Different design approaches for both load cases will be investigated by comparing the numerical results with the analytical results resulting from these approaches.

First, an overview will be given of the examined geometries and boundary conditions. Next, the existing design approaches for bending and the proposed approach for compression will be presented, together with the existing approaches in the European standards on which they are based. After this, an overview of earlier research of the authors concerning these approaches will be given. Subsequently, the finite element model used to examine the shown approaches will be described, after which a comparison will be made between the different approaches and the finite

element results. Based on this comparison, the design rules that agree best with the numerical results will be determined.

2. Examined geometries and boundary conditions

Cellular members are made by cutting a hot-rolled beam, the parent section, in two different halves according to the pattern depicted in Fig. 2. After the cutting process, which is usually an oxy-fuel cutting or a plasma cutting process, both halves are shifted relative to each other and welded together. In this process, there is a great flexibility in the possible geometries: it is possible that the top- and bottom part have different parent sections, which is very useful for composite beams. Furthermore, also tapered and even curved beams are easily fabricated by slightly adjusting the production process.

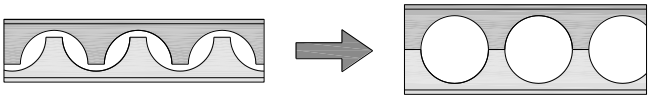

Figure 2. Fabrication of a cellular member starting from a plain-webbed parent section

In spite of the numerous different geometries, only the most basic sections were considered in this research: doubly symmetric beams, made from one parent section. For the parent sections, six European structural shapes were considered (Table 1). All feasible geometries starting from these parent sections were derived by varying the opening diameter, the width between the openings and the member length. The dimensions of each cross-section were checked using the constraints found in (CTICM, 2006). This way, a wide variety of realistic cellular beam geometries was obtained (220 per load case). In the following, the different groups of geometries will be referred to with their parent section name.

Table 1. Cellular beam parent sections

Examined parent sections					
IPE300	HE320M	HE320A	IEP600	HE650M	HE650A

For each geometry, comparisons will be made between the results of the different design approaches and the results from the finite element simulations. For these comparisons, only the basic cases of members with fork-supports at their ends, subjected to either a constant strong axis bending moment M or a normal compressive force N (Fig. 3) were considered. The axis conventions are as depicted in Fig. 3, with the x-as running along the length of the member, the y-axis being the strong axis and the z-axis the weak axis.

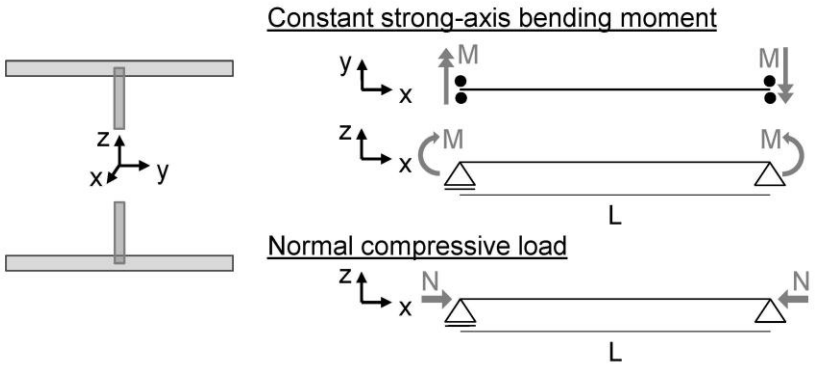

Figure 3. Axis conventions, considered load cases and boundary conditions

3. Design approach for cellular members – adaptation of the EC3 rules

In this section, an overview will be given of the existing and proposed design approaches for global buckling of cellular beams loaded by a constant bending moment (M) or a compressive force (N). The governing buckling modes in these cases are respectively lateral-torsional buckling (LTB) and weak-axis flexural buckling (FB_z) (Fig. 4). The proposed approaches are based on the design rules for plain-webbed beams that can be found in the European Standard EN 1993-1-1 (CEN, 2005), which will be further referred to as EC3 (Eurocode 3). An overview of the original EC3 rules valid for beams without web openings will be given, discussing the specific adaptations for cellular members.

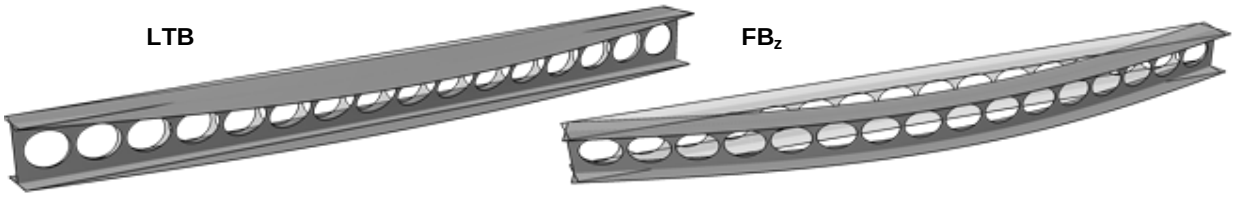

Figure 4. LTB and FB_z buckling modes

3.1 Design approach for cellular members

In this part, an overview will be given of the basic design approaches for LTB and FB_z failure of cellular members.

3.1.1 Approach for LTB

The global buckling mode for a beam loaded in bending is lateral-torsional-buckling (LTB). Currently, two different approaches exist to calculate the LTB failure moment of a beam loaded in bending. According to the first approach (CTICM, 2006), the LTB failure should be considered as the flexural buckling (FB) failure of the compressed tee-section at the opening (Fig. 5). Since the torsional stiffness of the section is completely neglected, this approach is very conservative. The second approach is based on the findings in (Nethercot, 1982), and is included in an annex of the European pre-standard ENV 1993-1-1 (CEN, 1992), which will be further referred to as ENV3. According to this approach, the LTB failure moment can be calculated in the same way as for a plain-webbed member, but by using the cross-sectional properties calculated at the central position of the opening. This approach, only being very concisely mentioned in ENV3, was further expanded in a wider European research project about LTB of beams (Maquoi, 2003).

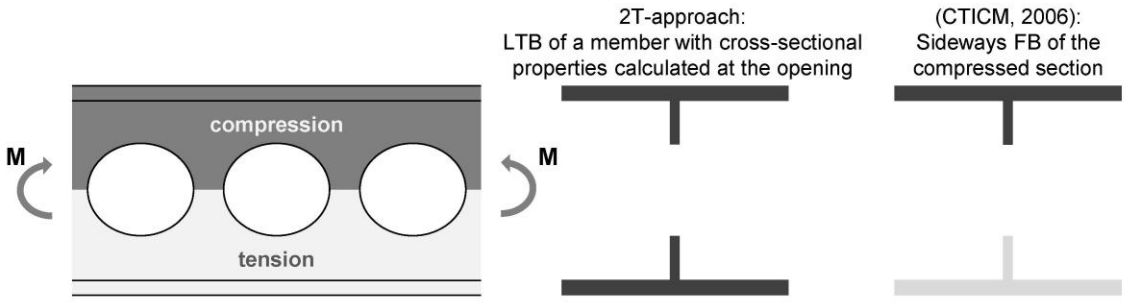

Figure 5. The two existing design approaches for LTB of cellular beams

In a preliminary study, the authors have compared the elastic critical (bifurcation) moment M_{cr} obtained using both approaches with the results of linear buckling simulations in Abaqus (Sonck, 2009b). In this work, it was shown that the first approach (from the CTICM) was very conservative. As a result, only the second approach will be further examined in this paper. The latter approach will be further referred to as the 2T-approach, because the cross-section at the opening consists of two T's, placed opposite each other (Fig. 5).

3.1.2 Approach for FB_z

The governing global buckling mode for the considered simply supported, doubly symmetric, compressed members is weak-axis flexural buckling (FB_z). For this failure mode no design approaches exist, according to the authors' best knowledge. It is proposed that the 2T-approach, already existing for LTB failure of cellular members, is used for FB_z failure as well.

3.2 Adapted EC3 rules

In the following, a short overview of the EC3 rules will be given, together with the specific adaptations that are needed for the 2T-approach proposed for cellular members. Because the EC3 rules for LTB are based on the rules for FB, the latter rules will be given first.

3.2.1 Adapted EC3 approach for FB_z

According to EC3, the buckling verification of a member loaded in compression is expressed by Eq. 1, in which N_{Ed} is the design value of the compressive force and $N_{b,Rd}$ is the design buckling resistance of the compression member.

$$\frac{N_{Ed}}{N_{b,Rd}} \leq 1 \tag{1}$$

The design buckling resistance of a compression member can by calculated as follows:

$$N_{b,Rd} = \frac{N_{b,Rk}}{\gamma_{M1}} = \frac{\chi A f_y}{\gamma_{M1}} \tag{2}$$

In Eq. 2, A is the cross-sectional area; f_y is the yield stress and χ the reduction factor for the relevant buckling mode. The factor γ_{M1} is a partial factor that should be applied to the characteristic value of the buckling resistance $N_{b,Rk}$. For buildings, it is recommended that the value of γ_{M1}=1.0 is used. In Eq. 2, the full plastic cross-sectional capacity Af_y is used. Since reductions in this capacity due to local buckling are not taken into account, this equation is only valid for class 1, 2 or 3 cross-sections according to EC3. In the adapted rules for cellular members, it will be assumed that the full plastic resistance of the cross-section can be used without local buckling effects. This corresponds with the results found in the numerical simulations. However, it is possible that for some geometries, other than the examined, the full plastic resistance cannot be used. Further research will be needed to examine this as well.

The reduction factor χ can be calculated using the relevant buckling curve, in which χ is expressed as a function of the non-dimensional slenderness $\bar{\lambda}$ (Eq. 3).

$$\bar{\lambda} = \sqrt{\frac{A f_y}{N_{cr}}} \tag{3}$$

The critical load N_{cr} is the elastic critical (bifurcation) load for the relevant buckling mode. For the considered geometries and boundary conditions, the governing global buckling mode will be weak-axis flexural buckling and the critical buckling load can be expressed by Eq. 4.

$$N_{cr,z} = \frac{\pi^2 EI_z}{L^2} \tag{4}$$

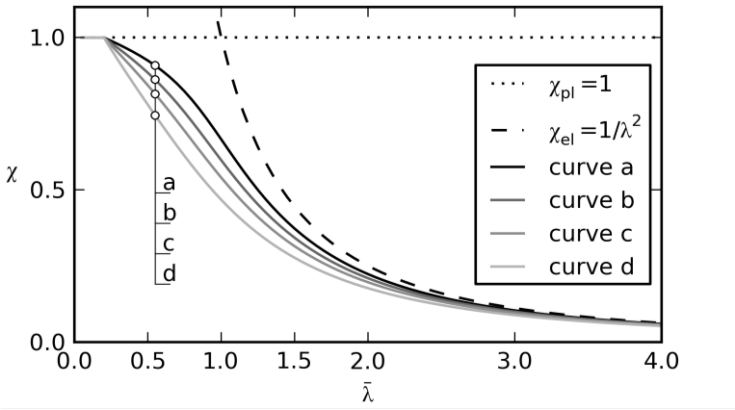

Figure 6. Buckling curves according to EC3

The buckling curves represent the influence of residual stresses and geometric imperfections on the buckling failure behavior of the member. As can be seen in Fig. 6, these influences are most pronounced for intermediate values of the slenderness $\bar{\lambda}$ (between 0.5 and 1.5). For low values of $\bar{\lambda}$, χ approaches the "plastic" value 1, i.e. $N_{b,Rd}=Af_y$. For high slendernesses, χ approaches the "elastic" value χ_{el} (Eq. 5), where $N_{b,Rd}=N_{cr}$.

$$\chi_{el} = \frac{1}{\bar{\lambda}^2} \tag{5}$$

Table 2 shows the weak-axis flexural buckling curve limits that are relevant for the geometries used in this paper. Details for other geometries can be found in EC3. The depth-to-width ratio h/b of 1.2 corresponds with the h/b-boundaries for the different residual stress patterns that were assumed for members with an h/b-ratio larger or smaller than 1.2 (Fig. 7) in the determination of the buckling curves (ECCS, 1984).

Table 2: Buckling curve selection for weak-axis FB (Valid for steel grade S235)

	Buckling curve
h/b≤1.2 and tf≤100mm	c
h/b>1.2 and tf≤40mm	b

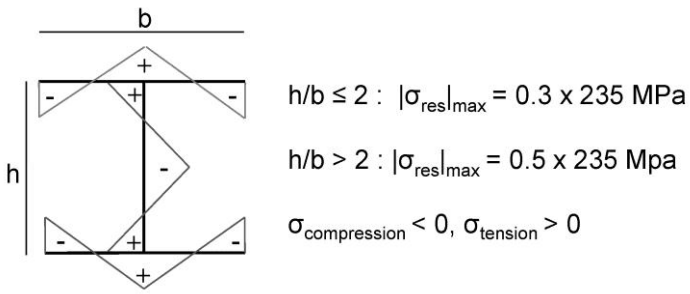

Figure 7: Residual Stresses according to (ECCS,1984) for hot-rolled sections

For cellular members, additional assumptions concerning the buckling curves are needed. In order to decide which curves to use, two factors are taken into account. Firstly, the choice of the buckling curve in EC3 complies with the different residual stress patterns assumed in the determination of the buckling curves. Secondly, it can be assumed, as an initial approximation, that the residual stress pattern does not change considerably during the production process (cf. §5 for more details). Taking both factors into account, for FB_z it is proposed that the same buckling curve should be used for the cellular members as for their parent section.

3.2.2 Adapted EC3 approach for LTB

According to EC3, the resistance of a beam against LTB is sufficient if Eq. 6 is valid, with M_{Ed} the design value of the bending moment and $M_{b,Rd}$ the corresponding design buckling resistance. The value of $M_{b,Rd}$ can be calculated by Eq. 7. In this expression, W_y is the appropriate strong-axis section modulus, depending on the cross-section class. For cellular members, the plastic section modulus $W_{y,pl,2T}$ was used for all geometries, which was justified by the numerical results.

$$\frac{M_{Ed}}{M_{b,Rd}} \leq 1 \tag{6}$$

$$M_{b,Rd} = \frac{M_{b,Rk}}{\gamma_{M1}} = \frac{\chi_{LT} W_y f_y}{\gamma_{M1}} \tag{7}$$

The influence of residual stresses and imperfections is represented by the reduction factor χ_{LT}. This value can be calculated using the relevant buckling curve. In EC3, two different methods are given to calculate the buckling curve: the so-called "general method" and the "specific method". In this work, the "general method" will be used, in which the same buckling curves as for FB are prescribed, this formulation also being utilized in (Maquoi, 2003). Furthermore, the "specific method" is still the subject of discussion, this method being less conservative and even unsafe for some cases (Rebelo, 2008)

The non-dimensional slenderness $\bar{\lambda}_{LT}$ can be determined by Eq. 8. The elastic critical (bifurcation) moment M_{cr} of a member with fork-supports, loaded by a uniform bending moment, can be calculated according to Eq. 9. In this expression L is the length of the member, GI_t the torsional stiffness of the cross-section, EI_z its strong-axis bending stiffness and EI_w its warping stiffness.

$$\bar{\lambda}_{LT} = \sqrt{\frac{W_y f_y}{M_{cr}}} \tag{8}$$

$$M_{cr} = \frac{\pi}{L}\sqrt{GI_t EI_z + \frac{\pi^2}{L^2} EI_z EI_w} \tag{9}$$

The buckling curves that should be used according to EC3 are given in Table 3, with h the total depth of the cross-section and b the cross-section width. The depth-to-width ratio h/b should take the different LTB failure behavior of slender (h/b>2) vs. stocky sections into account.

Table 3: Buckling curve selection for LTB according to EC3 (rolled sections)

	Buckling curve
h/b≤2	a
h/b>2	b

The lateral-torsional buckling curve formulation is identical to the formulation for flexural buckling, the only difference between both being the rules that define which buckling curve should be used for which section (e.g. Tables 2 and 3). In contrast with the buckling curve used for FB, no explicit mechanical background exists for the LTB curves. Recently, criticism has risen against the fact that there is no consistent mechanical derivation for the LTB buckling curve (Taras, 2010a and 2010b). This causes the depth-to-width ratio to be an approximate representation of a variety of effects which play a role in the LTB behavior, such as the torsional stiffness and the behavior in plasticity. Because of this, the LTB curves are less precise than the FB curves. Additionally, it is confusing that the role of the residual stresses is not clear to the designer, as opposed to what is the case for FB, where the residual stresses are directly connected to the given h/b-ratios. However, this paper will only go as far as the mentioning of these issues, and no attempts for improvement of the LTB curves formulations will be made.

For cellular members, additional assumptions concerning the buckling curves are needed. In (Maquoi, 2003), it was proposed that the values from Table 3 are used, with h now being the total height of the cellular member. Reduction factors thus calculated will be referred to as $\chi_{a/b}$. Additionally the results from the finite element simulations will be also compared with the results using the $\chi_{b/c}$ formulation, which are one buckling curve lower. Because the h/b-boundaries are slightly artificial, the numerical results will also be compared with the reduction factors using curve b or c for all geometries (respectively χ_b and χ_c). The use of buckling curve c corresponds with what is proposed in (Nseir, 2012).

4. Earlier research of elastic buckling of cellular members

In earlier research, the authors have compared finite element simulation results with results from the 2T-approach for the critical load (Sonck 2010a and 2010b). Using the same parent sections as in the research in this paper (Table 1), a large variety of cellular member geometries was derived for which the results could be compared. In this section the results of this comparison will be shown for M_{cr} and $N_{cr,z}$.

4.1 Critical LTB moment M_{cr}

In (Sonck, 2010a), the analytical expression for M_{cr} was compared with FE results. All investigated members failed by global buckling. In the left of Fig. 8, the value of the critical moment obtained from the finite element simulations ($M_{cr,abq}$) is compared with the critical moment obtained using the 2T- approach ($M_{cr,2T}$). On the vertical axis, the percent error of the 2T-approach compared to the finite element results is given, and along the horizontal axis the length of each examined geometry is shown. For most geometries, the results obtained using the 2T-approach were safe ($M_{cr,2T}<M_{cr,abq}$) or just very slightly unsafe.

However, for the short length geometries with a HE320M or HE320A parent sections, larger unsafe deviations could be perceived. This is due to the web distortion that was observed for these specific sections (Fig. 8, right). Web distortion and the accompanying decrease in stiffness occur due to an interaction between local buckling of the cross-section and global LTB, for relatively short length members with relatively slender webs. More details about this can be found in (Bradford, 1992) and (Schafer,2005). This behavior is not very important for elastic buckling of normal hot-rolled members, due to the limited slenderness of their web, but in (Sonck, 2009a), it was found that the web distortion will be larger for cellular members than for

members without openings. However, it is expected that in reality, the failure of the affected short-length members will be governed by plastic yielding instead of elastic buckling. Accordingly, the detrimental effect that was observed for the elastic critical moment will not influence the failure load substantially. The influence of the plastic behavior was already shortly investigated by the authors in (Sonck, 2011a), where it was found that this was indeed the case.

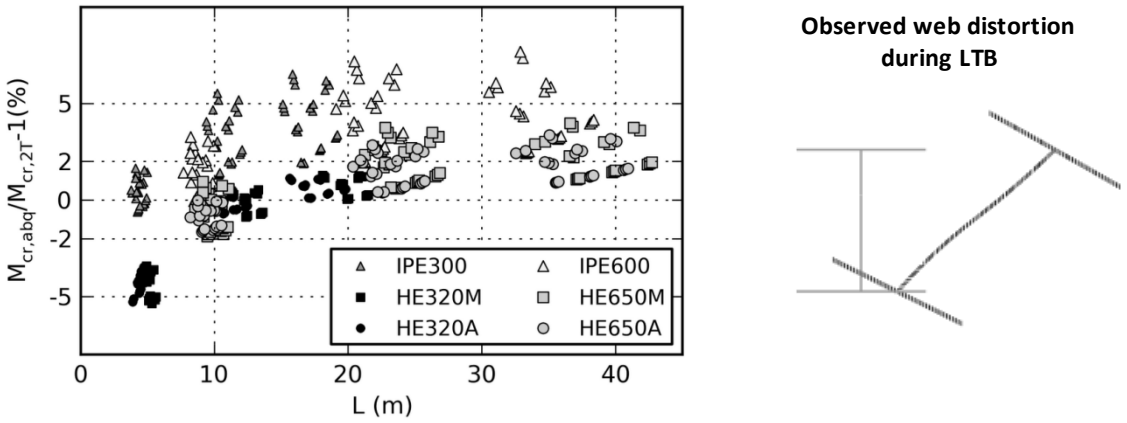

Figure 8. comparison of the 2T-approach with numerical results for M_{cr} (left), web distortion during LTB (right)

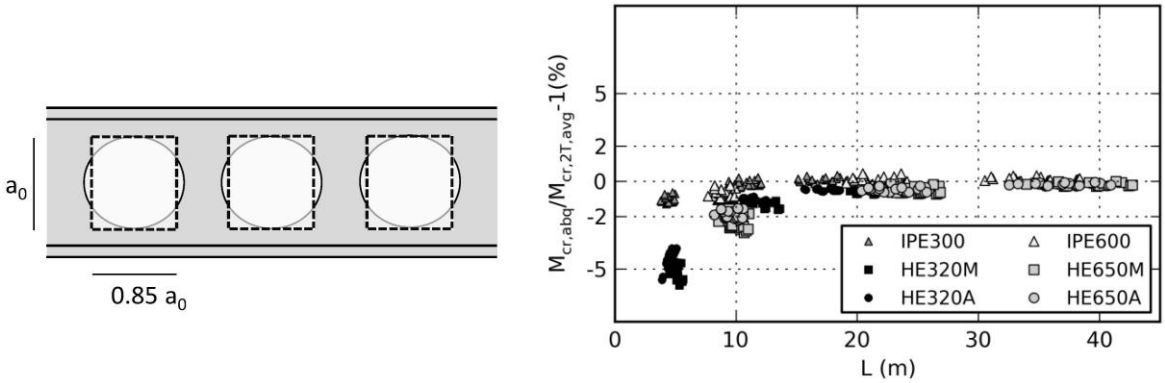

Figure 9. Weighted average approach for M_{cr}: rectangular opening approximation (left), comparison with numerical values (right)

In Fig. 8, one can see an underestimation of the critical moment for the larger lengths, especially for the members with IPE300 or IPE600 parent sections. As the research in (Vancaeyseele,2010) shows, this is caused by an underestimation of the torsional stiffness GI_t, of which the effect increases for increasing lengths. While this underestimation is safe, it was tried to diminish these deviations by using a modified weighted average approach. According to this approach, the value of the St. Venant torsion constant $I_{t,avg}$ of a cellular beam is found by calculating the weighted average torsional constant of a beam with rectangular openings as drawn in Fig. 9. The expression for $I_{t,avg}$ is given in Eq. 15, with $I_{t,full}$ the torsional constant of the beam section without an opening, $I_{t,2T}$ the torsional constant at the opening, L the length of the beam and n the number of openings In this weighted average, the relative length of the rectangular openings is the weight of $I_{t,2T}$ and the relative length of the sections without openings is the weight of $I_{t,full}$.

$$I_{t,avg} = \frac{0{,}85 a_0 n}{L} I_{t,2t} + \left(1 - \frac{0{,}85 a_0 n}{L}\right) I_{t,full} \tag{15}$$

Using $I_{t,avg}$ for the torsional constant and the 2T-approach for the remaining cross-sectional properties, the critical moment $M_{cr,2T,avg}$ could be calculated and compared with the finite element results. As can be seen in Fig. 9, the deviations that existed for the longer geometries have almost completely disappeared.

4.2 Critical FB_z load (N_{cr})

Analytical results for the 2T approach were also compared with finite element results for the critical load for compressed cellular members (Sonck, 2010b). In the simulations, all investigated members failed by flexural buckling. The results of this comparison are shown in Fig. 10. The numerical results ($N_{cr,abq}$) correspond quite well with the analytical expression using the 2T-approach ($N_{cr,2T}$). Only for the short-length members with HE320A and HE320M parent sections, some small unsafe deviations can be observed, again due to web distortion (right of Fig. 10). However, these deviations are very small and additionally, it is expected that these will be again rendered insignificant if the effects of plasticity are taken into account.

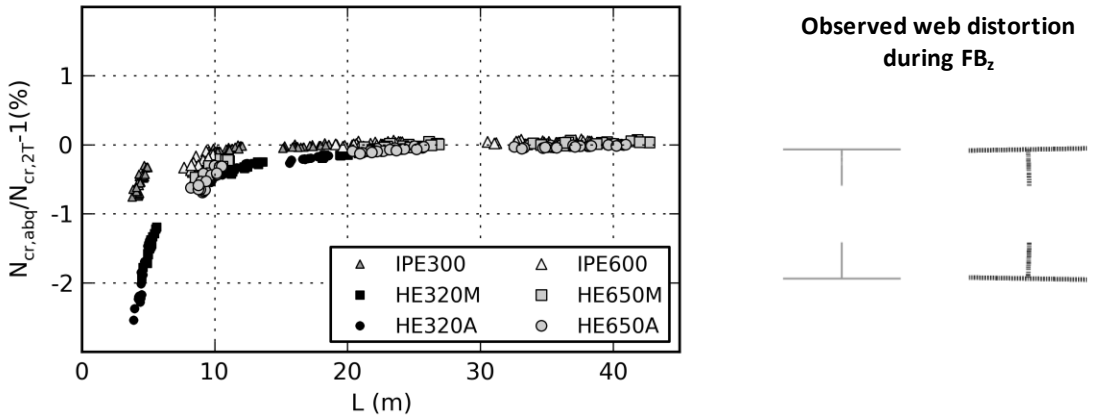

Figure 10. comparison of the 2T-approach with numerical results for N_{cr} (left), web distortion during FB_z (right)

5. Numerical simulations

In this work, the resistance formulations for the global buckling failure of cellular members loaded in bending or compression will be compared with results from numerical simulations in Abaqus. Compared to the work described in §4, additional effects of geometric and material nonlinearities, as well as imperfections will now be taken into account as well.

5.1 Finite Element model

The ultimate failure moment or failure compressive force was calculated with the finite element package Abaqus. A geometrically nonlinear analysis taking into account nonlinear material behavior and imperfections was performed using the modified Riks method, an arc length technique. The member is loaded in compression or bending, and the maximum load that the member can carry is considered as the failure load.

The geometry was modeled using quadratic shell elements with reduced integration (S8R) for both the flanges and the webs. The fillet between the flanges and the webs was not taken into account, both in the numerical model as in the theoretical expressions. The used boundary conditions were those of the classical LTB setup: a beam with fork-supports, which means that the torsional rotation of the beam ends is prevented, without preventing the warping.

Additionally, the beam is simply supported (Fig. 2). The uniform strong-axis bending moment and the compressive force were applied at both beam ends by means of line loads acting on the flanges and the web. Local deformations due to boundary conditions or load application were prevented by using kinematic coupling constraints that impose that the cross-section keeps its shape at the ends.

5.2 Non-linear material behavior

As material, only steel of grade S235 was considered, modeled by a bilinear stress-strain curve without strain hardening, with a Young's modulus of 210 GPa and a yield stress of 235 MPa. The reduction of the yield stress that occurs for larger material thicknesses was not taken into account, both in the numerical model as in the theoretical approach. The used Poisson's ratio of the elastic steel was 0.3.

5.3 Imperfections

Both geometric imperfections and residual stresses were applied in the model. As geometric imperfection, a half-sine wave with amplitude L/1000 was chosen in both the FB and LTB simulations, as a first approximation. This corresponds with the amplitude that was originally used to determine the buckling curve values of the ECCS. Only an out-of-plane imperfection (in strong axis direction) was applied (Fig. 12). Nevertheless, it is possible that this imperfection alone will not be sufficient and local imperfections typical for cellular members will have to be introduced as well. This will be further investigated in the future.

It is assumed that the parent sections have a residual stress pattern in the flanges that corresponds with the ECCS recommendation, given in Fig. 6, this pattern also being used in the finite elements simulations for the derivation and calibration of the original FB buckling curves. For reasons of simplicity, the residual stresses in the webs were set equal to zero (Fig. 11), the residual stresses in the flanges being dominant for the considered LTB or FB behavior.

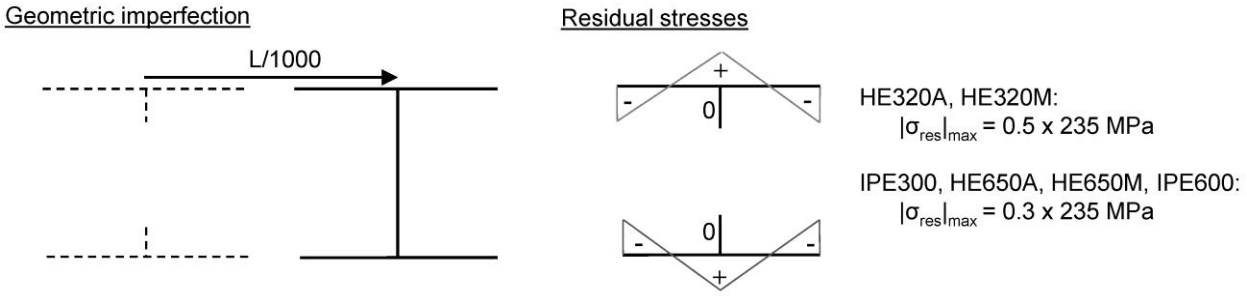

Figure 11. Used Imperfections

However, some uncertainties exist about the assumed nominal imperfection values. Firstly, it is possible that the residual stresses in the flanges are affected detrimentally by the effects of the cutting of the beam and the welding of the beam halves. Both processes could result in an increase of the compressive stresses in the flange, which has a detrimental effect on the failure behavior in LTB or FB. Additionally, the magnitude and shape of the geometric imperfections could be changed considerably by the production process, which can have a detrimental effect on the failure load. Further experiments and finite elements simulations will be needed to

investigate both uncertainties in the future. Nevertheless, the used approach should be considered as a good first approximation of the failure behavior.

5.4 Determination of failure load

In the numerical analyses, all members failed by global buckling: LTB or FB, respectively for the members loaded in bending or compression. Since no local buckling effects were observed, it seems that the assumption to use the full plastic resistance in the design formulations seems reasonable.

For each examined geometry, a load-displacement curve can be determined using the results from the GMNIA analysis. Using the maximum value of the load that was reached during the Abaqus simulation ($N_{max,abq}$ or $M_{max,abq}$), the value of χ_{abq} can be calculated using Eq. 2 or Eq. 7 with respectively $N_{b,Rd}=N_{max,abq}$ or $M_{b,Rd}=M_{max,abq}$. In the following section, the values of χ_{abq} will be compared with the different design approaches.

6. Comparison of results

In this section, the results from the various design approaches will be compared with the results of the finite element simulations. For each geometry, the theoretical slendernesses $\overline{\lambda}$ or $\overline{\lambda}_{LT}$ using the 2T-design approach can be defined from respectively Eq. 3 or 8.

6.1 Flexural Buckling

Only one design approach will be examined for the FB_z failure of cellular members. As mentioned in §3.2.1, the results of the finite element simulations for the HE320A and HE320M parent sections should be compared with curve c, while the results for the other parent sections should be compared with curve b. The influence of the residual stresses on the buckling curve is quite clear in the left graph of Fig. 12, where it can be seen that the HE320A and HE320M groups clearly correspond with a lower buckling curve than the members with the remaing parent sections. As can be seen in Fig. 12 and Table 4 , the overall agreement is quite good. For the short length HE320M, some unsafe deviations can be observed. It is unlikely that this is due to web-distortion, because the influence of the distortion should be similar for the HE320M and the HE320A groups, while for the latter group of geometries the unsafe deviations are much smaller. More research will be needed to give a sound explanation for the unsafe deviations of the short length HE320M geometries.

Table 4. Deviations of design approach compared with numerical results for FB

	IPE300	HE320M	HE320A	IEP600	HE650M	HE650A	ALL
Minimum Δ_{2T} (%)	-2	-7	-2	-1	-1	-1	-7
Maximum Δ_{2T} (%)	8	7	7	8	8	8	8
Mean Δ_{2T} (%)	4	3	4	4	4	4	4

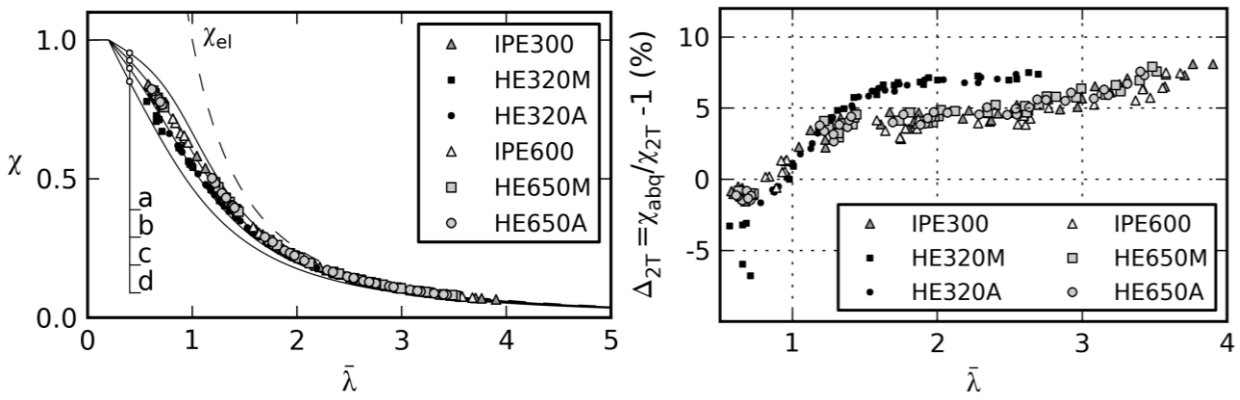

Figure 12. Comparison of numerical results with design approach for FB

6.2 Lateral-torsional buckling

In Fig. 13, the comparison between the calculated $\left(\overline{\lambda}_{LT,}\chi_{abq}\right)$and the buckling curves for LTB for each examined geometry is made. As can be seen, the obtained results follow the buckling curve shape. The lowest results (HE320A) lie above curve c, while the highest results (HE320M) are positioned higher than buckling curve a.

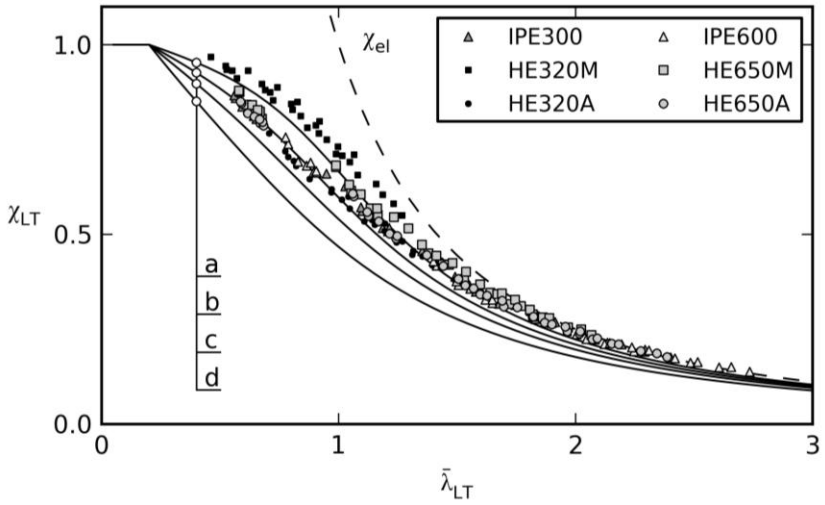

Figure 13. Buckling curve comparison of numerical results with design approach for LTB

The depth-to-width factor h/b of the cellular member is smaller than the boundary value of 2 for the cellular members with HE320M and HE320A parent sections, and larger than 2 for all other members. Subsequently, it was expected that the results of the former group of cellular members should correspond with the highest buckling curves and the results of the latter groups with the lowest. The HE320A results strongly deviate from these expectations, already giving an indication that the proposed h/b boundaries and possibly also the buckling curve formulation should be altered.

In Fig. 15 and 16, the deviation between the numerical results and the results from different design approaches are presented in function of the slenderness. The numerical values of the

minimum, maximum en mean deviations for each parent section are shown in Tables 5-7. In Fig. 14, the results are shown for buckling curves a/b ($\chi_{a/b}$) or b/c ($\chi_{b/c}$). It can be seen that the $\chi_{a/b}$ approach, which was proposed in (Maquoi, 2003) gives considerably unsafe results for the HE320A group (up to -14%). For all other sections, the results range from slightly unsafe to safe, the maximum value of the deviation being 23% for the HE650M section. If the $\chi_{b/c}$ approach is used, the unsafe deviations for the HE320A group decrease to -4%, while the safety for the other parent sections increases to 33%.

Table 5. Minimum deviation values for each parent section group

Minimum values	$\Delta_{a/b}$ (%)	$\Delta_{a/b,avg}$ (%)	$\Delta_{b/c}$ (%)	$\Delta_{b/c,avg}$ (%)	Δ_{b} (%)	Δ_{c} (%)
IPE300	-1	-1	6	6	-1	6
HE320M	1	1	7	7	7	12
HE320A	-14	-14	-4	-5	-4	5
IPE600	-2	-2	7	7	-2	7
HE650M	1	1	8	8	1	8
HE650A	-1	-1	6	6	-1	6
Minimum	-14	-14	-4	-5	-4	5

Table 6. Maximum deviation values for each parent section group

Maximum values	$\Delta_{a/b}$ (%)	$\Delta_{a/b,avg}$ (%)	$\Delta_{b/c}$ (%)	$\Delta_{b/c,avg}$ (%)	Δ_{b} (%)	Δ_{c} (%)
IPE300	21	15	29	23	21	29
HE320M	14	13	28	26	28	41
HE320A	8	7	17	15	17	27
IPE600	20	14	27	21	20	27
HE650M	23	19	33	29	23	33
HE650A	19	15	27	23	19	27
Maximum	23	19	33	29	28	41

Table 7. Mean deviation values for each parent section group

Mean values	$\Delta_{a/b}$ (%)	$\Delta_{a/b,avg}$ (%)	$\Delta_{b/c}$ (%)	$\Delta_{b/c,avg}$ (%)	Δ_{b} (%)	Δ_{c} (%)
IPE300	11	9	19	17	11	19
HE320M	7	6	17	16	17	27
HE320A	-4	-5	5	5	5	15
IPE600	10	8	19	16	10	19
HE650M	14	12	24	22	14	24
HE650A	10	9	19	18	10	19
Mean	9	7	18	16	5	21

On the right side of Fig. 14, the results using the weighted average-2T-approach are shown. In this approach, the values of $\overline{\lambda}_{LT,avg,}$ and $\chi_{a/b,avg}$ or $\chi_{b/c,avg}$ are all calculated using $I_{t,avg}$ for the torsion constant and the 2T-approach for all other section properties. For the IPE600 group, for which the largest improvement in M_{cr} was noticeable using this approach instead of the 2T-approach, the influence of the approach can be seen most clearly. However, compared to the total deviations for the buckling resistance moment, the effect of this approach is rather small. As long as these large deviations are not reduced, the small effect of the weighted average-2T-approach is negligible. As a consequence, this approach will not be used in the further comparisons. Nevertheless, once the overall deviations can be decreased by an improved formulation of the buckling curves for LTB, this approach could become more valuable.

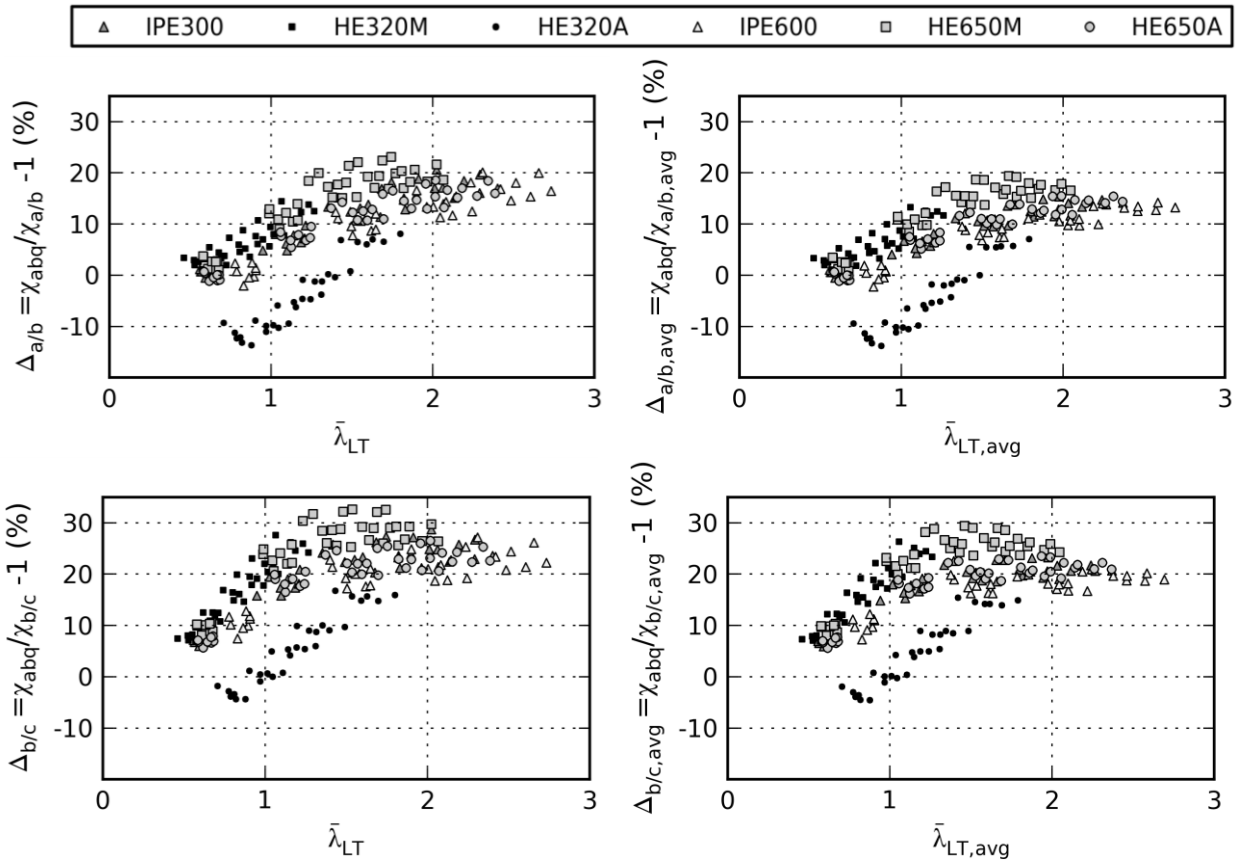

Figure 14. Comparison of 2 buckling curve approach

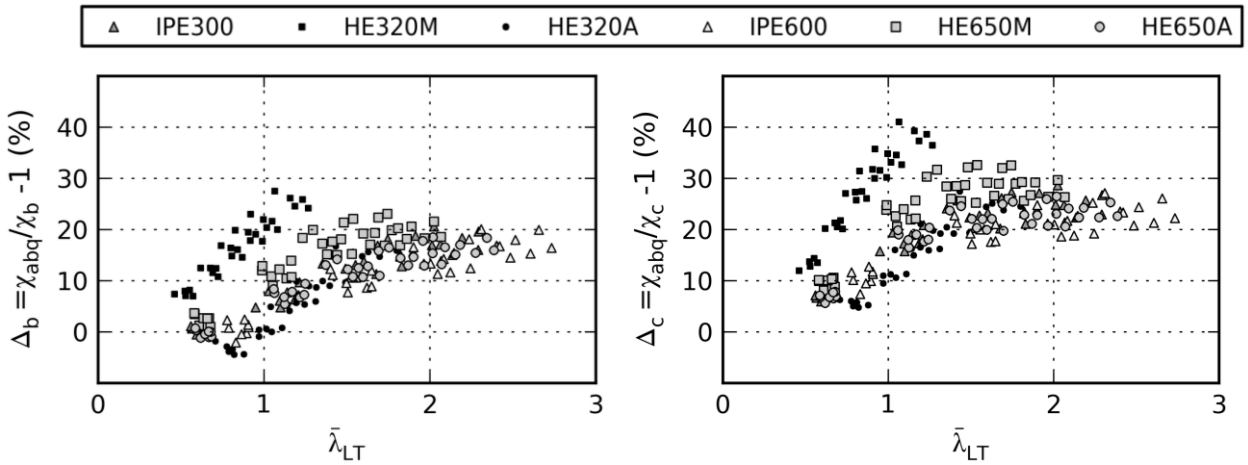

Figure 15. Comparison of 1 buckling curve approach (b and c)

In Fig. 15, a comparison is shown between the numerical results and the results using buckling curve b or c for all sections. For curve b, the minimal deviation is -4% for the HE320A parent section, while the maximum deviation is 28%. The results for curve c are always safe, with the minimal deviation being 5% for the HE320A prent section, and the maximum deviation 41%. From all examined approaches for LTB of cellular beams, the results from the 2T-approach with curves b and c for, independent of h/b, approximate the numerical results the best.

In (Nseir, 2012), similar comparions between numerical simulations and the 2T-design approach were made for the LTB failure. In the finite element model, residual stresses were neglected, which was countered by larger geometric imperfections of various shapes (both local and global). In this work, it was found that buckling curve c gave optimal results. The examined geometries and the assumed imperfection being different in both investigations, there is certainly an agreement between the results of this work and (Nseir, 2012). The slightly lower numerical values (and the lower resulting buckling curve c) can be attributed to the larger geometric imperfections amplitudes that were used in the latter work.

The differences in the assumed geometric imperfections and residual stresses in this work and (Nseir, 2012) demonstrate the large uncertainties regarding the values of both imperfections that should be assumed in the numerical modelling of cellular beams. These uncertainties can only be solved by doing more detailed research on both imperfection types. This lack of knowledge becomes even more stringent when the reliability of the design rule will have to be calculated using a probabilistic method, for which information about the statistical distributions of both imperfections will be needed.

7. Conclusions

In this paper, different design approaches to check the global buckling resistance of a cellular member loaded in bending or compression are presented. All examined approaches are based on the 2T-approach, in which the resistance of the cellular member can be calculated in the same way as the resistance of a member without web openings, but with all cross-sectional properties calculated at the weakest cross-section. For cellular members loaded in bending, this approach already existed, although it was unclear which buckling curve would be more suited to calculate the reduction factor, or, alternatively put, how large the influences of the different imperfections should be chosen in this approach. To date, no relevant studies were available for compressed cellular members, and it was proposed that the approach for bending should be used as well for this case.

This approach had already been examined in previous work for the elastic critical load in bending or compression, by comparing its results with numerical simulations for a wide variety of cellular beam geometries. It was found that the agreement between this approach and the numerical values was good, but that for some short length geometries the results were slightly unsafe because of web distortion. However, it was expected that these unsafe deviations would vanish once the plastic behavior of the beams was taken into account.

In this work, the additional effect of imperfections, as well as material and geometric nonlinearities on the failure behavior was determined by comparing the finite element results with the proposed design rules for the buckling resistance. For compressed cellular members, only one approach was examined, in which the 2T-approach was combined with the buckling curves of the original parent sections. This approach gave very satisfactory results. However, it should be taken into account that the results are only valid if the preliminary assumptions for residual stresses and imperfections are proved to be correct.

For failure of cellular members loaded in bending, the results using the 2T-approach paired with buckling curve b or c for all parent sections, regardless of h/b, approximate the numerical results

the best. However, improvements are possible for both approaches, buckling curve b being slightly unsafe, while curve c is maybe already too safe. Before the process of looking for these improvements and refining the different buckling curve formulations even can be commenced, the mentioned uncertainties concerning the assumed imperfections (geometric and residual stresses) will need to be clarified. Additionally, the recently arisen issues for LTB of beams without web openings will have to be resolved as well.

In future research, the residual stress pattern will be examined in more detail, using numerical simulations and experiments. Additionally, bending and compression experiments will be conducted to study the FB and LTB behaviour. In these experiments, the imperfections will be further studied as well. Furthermore, the combined M+N load case as well as more realistic boundary conditions will be investigated numerically.

Acknowledgments
The authors would like to thank Huys Liggers (Venlo, Holland) for supplying the cellular members that will be used in the future experiments of this paper.

References

Bradford M.A. (1992). "Lateral-distortional buckling of steel I-section members". *Journal of Constructional Steel Research*, Elsevier, 23, 97-116.

CEN (1992). "ENV 1993-1-1. Eurocode 3: Design of steel Structures. Part 1-1: General rules and rules for buildings. Annex N: Openings in webs". CEN (European Committee for Standardization), Brussels

CEN (2005). "EN 1993-1-1. Eurocode 3: Design of steel Structures. Part 1-1: General rules and rules for buildings". CEN (European Committee for Standardization), Brussels

CTICM (2006). "ARCELOR Cellular Beams-Detailed Technical Description (Technical documentation for software ARCELOR Cellular Beams v2.32)". CITCM (Centre Technique Industriel de la Construction Métallique), France.

Maquoi R., Heck C., de Ville de Goyet V., Braham M., Richard C., Müller C. et al. (2003). "Research project 7210-PR-183. Final Technical Report: Lateral-torsional Buckling in Steel and Composite Beams. Book 2: Design Guide." European Commission Directorate-General for Research , Luxembourg

Nethercot D. A., Kerdal D. (1982). "Lateral-torsional buckling of castellated beams". *The Structural Engineer*. 60B(3), 53-61

Nseir J., Lo M., Sonck D., Somja H., Vassart O., Boissonnade N. (2012). "Lateral Torsional Buckling of Cellular Steel Beams". *Proceedings of the Structural Stability Research Council Annual Stability Conference 2012*, Grapevine, Texas

Rebelo C., Lopes N., Simões da Silva L., Nethercot D., Vila Real P.M.M. (2008). "Statistical evaluation of the lateral–torsional buckling resistance of steel I-beams. Part 1: Variability of the Eurocode 3 resistance model" . *Journal of Constructional Steel Research*, Elsevier, 64, 818-831.

Schafer B.W., Adány S. (2005) "Understanding and classifying local, distortional and global buckling in open thin-walled members", Pr*oceedings of the Structural Stability Research Council Annual Stability Conference*, Montreal

Sonck D., Belis J., Lagae G., Vanlaere W., Van Impe R. (2009a). "Lateral-torsional buckling and lateral-distorsional buckling of I-section members with web openings". *Proceedings of the 8th National Congress on Theoretical and Applied Mechanics*, Brussels, Belgium, 406-411.

Sonck, D., Vanlaere, W., Lagae, G., Van Impe, R. (2009b). "Influence of web openings on failure by lateral-torsional buckling of cellular beams." *Proceedings of 15th Lightweight Structures in Civil Engineering (LSCE 2009) : Contemporary problems*, Warsaw, 170-173.

Sonck, D., Vanlaere, W., Van Impe, R. (2010a). "Elastic lateral-torsional buckling of cellular beams." *Proceedings of Steel Structures : Culture and Sustainability 2010*, Istanbul, 573-582.

Sonck, D., Vanlaere, W., Van Impe, R. (2010b). "Buckling of cellular members loaded by an axial force." *Proceedings of 2010 International symposium of the International Association for Shell and Spatial Structures (IASS 2010) : Spatial structures : temporary and permanent*, Shanghai, 1464-1471.

Sonck, D., Vanlaere, W., Van Impe, R. (2011). "Influence of plasticity on lateral-torsional buckling behaviour of cellular beams." *Materials Research Innovations*. Maney Publishing, 15(suppl. 1), S158-S161.

Taras A., Greiner R. (2010a). "New design curves for lateral-torsional buckling – proposal based on a consistent derivation." *Journal of Constructional Steel Research*, Elsevier, 66, 648-663

Taras A. (2010b). "Contribution to the development of consistent stability design rules for steel members". *PhD dissertation*, Graz University of Technology.

ECCS TC8-WG8.2 (Technical Committee 8 – Structural Stability Technical Working Group 8.2) (1984). "Ultimate Limit State Calculation of Sway Frames with Rigid Joints". *System Publication No. 33*, European Convention for Constructional Steelwork.

Vancaeyseele K. (2010). "Elastisch kip- en knikgedrag van cellulaire elementen." *Master thesis* (supervisors: Van Impe R., Vanlaere W.), Ghent University (in Dutch)

Westok, photograph of Porsche garage Liverpool, taken in January 2010 from Westok website. *www.asdwestok.co.uk/Applications/Columns/Porsche+Liverpool.htm*